

Anomalous shear viscosity-temperature behaviour of jojoba oil/LDH-stearate suspensions

W.W. Focke^{a,*}, L. Moyo^{a,#}, F.J.W.J. Labuschagne^a, N.G. Hoosen^a, S. Ramjee^a and M. Saphiannikova^b

^a Institute of Applied Materials, Department of Chemical Engineering, University of Pretoria, Private Bag X20, Hatfield, 0028, Pretoria, South Africa

^b Leibniz-Institut für Polymerforschung Dresden e.V., Hohe Strasse 6, Dresden D-01069, Germany

Abstract

Stearate intercalated layered double hydroxide was synthesized by reacting the corresponding carbonate form with a large excess of stearic acid. Thermal analysis, FTIR, XRD and SEM-EDS characterization indicated the formation of a highly crystalline bilayer-intercalated product. The composition of the inorganic portion showed high variability in the Al:Mg atom ratio. This suggests that the crystals comprised stacks of randomly interstratified layers that varied in compositions from one close to magnesium stearate to one similar to aluminium distearate. The rheology of the jojoba oil suspensions containing this material showed strong shear thinning behaviour and also an anomalous temperature dependence.

Keywords: Layered double hydroxide; Rheology modifier; Intercalation reaction; Electron microscopy

1. Introduction

Hydrotalcite is a natural anionic clay mineral $[\text{Mg}_6\text{Al}_2(\text{OH})_{16}\text{CO}_3 \cdot 4\text{H}_2\text{O}]$ [1]. Layered double hydroxides (LDHs) are its synthetic analogues [1-3] with variable magnesium to aluminium ratio as expressed in the molecular formula $[\text{Mg}_{1-\alpha}\text{Al}_\alpha(\text{OH})_2](\text{CO}_3)_{\alpha/2} \cdot x\text{H}_2\text{O}$ with $0.1 \leq \alpha \leq$

* Corresponding author. Tel.: +27 12 420 3728; Fax: +27 12 420 2516.

E-mail address: walter.focke@up.ac.za (W.W. Focke)

Current address: DST/CSIR National Centre of Nanostructured Materials, Council for Scientific and Industrial Research, Materials Science and Manufacturing, Pretoria 0001, South Africa

0.5 [4]. Both hydrotalcite and LDHs have a brucite-like $[\text{Mg}(\text{OH})_2]$ stacked sheet structure in which the cations are octahedrally coordinated by six oxygen atoms as hydroxides. The substitution of the Mg^{2+} with Al^{3+} ions imparts a net positive charge to the sheets. To compensate, the interlayers accommodate exchangeable charge-balancing anions and water. Thus the anionic exchange capacity (AEC) of these clays corresponds to α per LDH formula weight. The LDH- CO_3 precursor used in this study featured $\alpha \approx 0.316$, i.e. a magnesium to aluminium atom ratio of ca. 2.16.

Intercalation comprises a reversible insertion of a mobile guest species into a crystalline host lattice while maintaining the structural integrity of the latter [5]. Layered host lattices may adjust their interlayer separation in order to adapt to the packing geometry of the inserted guest species. Layered hosts usually feature strong intralayer covalent bonds and weaker interlayer interactions. LDH- CO_3 layers have a high charge density. The anionic species and water molecules present in the interlayer result in strong electrostatic and hydrogen bonding interactions between the sheets. They also impart substantial hydrophilic properties and ensure tight stacking of the lamellae. This hampers delamination of the stacks and exfoliation of the sheets in water and other solvents [6, 7]. The propensity to delaminate is improved by intercalation of linear organic molecules with appropriate functional groups. A wide range of anionic surfactants, including fatty acid salts, sulfonates, sulfates and phosphates are suitable for this task [7-10]. These long-chain molecules may self-assemble either as monolayers or as bilayers in the LDH galleries [8]. Such intercalated layered double hydroxides constitute a special class of nanostructured materials.

Nhlapo *et al.* [8] reported a surfactant-assisted intercalation method for the insertion of carboxylic acids into LDH- CO_3 powder suspended in water. Both anionic surfactants and nonionic surfactants aided bilayer intercalation of fatty acids. Thus, in the presence of water,

stearate ions are apparently able to displace carbonate ions from the layered double hydroxide galleries. The acidic fatty acid, e.g. stearic acid, reacts with the basic carbonate anions, CO₂ is released and the fatty acid is intercalated as a bilayer. The intercalation proceeds beyond the anion exchange capacity of the clay with the excess acid present in the undissociated form (R-COOH) [8]. In this study a nonionic surfactant was used to prepare stearic acid-intercalated LDH.

The chemical structure of jojoba oil differs from that of other vegetable oils. It is actually a polyunsaturated liquid wax composed of linear esters of fatty acids and straight chain alcohols. Both the acid and alcohol moieties typically feature 20 or 22 carbon atoms, and each has one unsaturated bond [11]. Jojoba oil melts at ca. 10 °C and thus it is a liquid at room temperature. It is more resistant to oxidation and to turning rancid than most other vegetable oils. The stability shown by jojoba oil makes it particularly useful for cosmetic applications [11]. Since its chemical composition resembles that of the skin's natural sebum, it is easily absorbed and rarely causes allergic reactions.

The purpose of this investigation was to determine the suitability of stearic acid-intercalated LDH as a thickening agent for jojoba oil for cosmetic applications. Towards this goal, the effect of stearate-intercalated LDH on the rheology of the jojoba oil was determined. It was found that the shear viscosity of such suspensions exhibited anomalous temperature dependence with the viscosity increasing with temperature in the range 20 °C to 40 °C.

2. Materials and methods

2.1. Materials

The layered double hydroxide (LDH-CO₃) was supplied by Chamotte Holdings. It contained silica and magnesium carbonate as minor impurities. Distilled water was used in all experiments. Other chemicals used were polyoxyethylene (20) sorbitan monostearate (Tween 60, Sigma); analytical grade stearic acid (Bio-Zone Chemicals), jojoba oil (100% pure cold pressed, Crede); magnesium stearate and aluminium stearate (Riedel-de Haën Product No. 26402).

2.2. Preparation of LDH-stearate

Several stearate intercalated layered double hydroxides (LDH-stearate) were prepared according to a method reported by Nhlapo *et al.* [8]. The standard procedure was as follows. A quantity of 20 g LDH-CO₃ and 40 g of surfactant (Tween 60) were dispersed in 1500 mL of distilled water preheated to 80 °C. Stearic acid (109.2 g, 0.384 mol), equivalent to about four times the AEC of the clay, was added in a three equal parts over a period of three days. The continuously stirred mixture was kept at 80 °C for 8 h and allowed to cool to room temperature overnight. The pH of the mixture was maintained at 9.5 ± 0.5 by adding ammonia solution, with a correction carried out once each day. On the fourth day the same procedure was followed except that no acid was added. On the next day the solids were separated by centrifugation, washed once with water and three times with ethanol and finally once with acetone. The recovered LDH-stearate solids were dried at room temperature. This product was the primary material investigated in this study and it is denoted as LDH-(4)-stearate. The same procedure was executed using half the amount of stearic acid to obtain the corresponding LDH-(2)-stearate product.

The above procedure was repeated in the absence of any stearic acid. This was done to determine whether the Tween 60 could intercalate into the LDH-CO₃ on its own. Finally, a

2:1 molar mixture of magnesium stearate and aluminium stearate was reacted using a very similar process. A quantity of 40 g Tween 60, 28.38 g (0.048 mol) magnesium distearate and 21.06 g (0.024 mol) aluminium tristearate were suspended in 1000 mL distilled water and heated to 70 °C. As before, ammonia solution was added to control the pH. The product was recovered as described above. The yield of this product denoted LDH-(5)-stearate, was 78.7%.

2.3. Preparation of organomodified LDH-jojoba oil dispersions

Preliminary investigations showed that the jojoba oil dispersion should contain at least 20 wt.% LDH-(4)-stearate and be heated to 80 °C otherwise the oil eventually bleeds out from the weak gel that forms. For the present investigation 30 wt.% LDH-(4)-stearate was selected unless otherwise indicated. A typical procedure was as follows. A quantity of 3 g LDH-(4)-stearate and 7 g jojoba oil were added to a glass beaker. The dispersion was heated to 80 °C in a hot water bath. It was continuously stirred with a glass rod until it was well mixed. The mixture was allowed to cool down to room temperature overnight. The 30 wt.% magnesium stearate and 30 wt.% aluminium stearate formulations were prepared according to same procedure by replacing the 3 g LDH-(4)-stearate with 3 g magnesium stearate and 3g aluminium stearate respectively.

2.4. Characterization

A small quantity of the LDH-stearate or the LDH-CO₃ precursor powder was placed onto carbon tape on an aluminium sample holder. Excess powder was removed using a single

compressed air blast. These powder samples were viewed either on a JEOL 840 JSM SEM scanning electron microscope.

Samples for XRF analysis were ground to $<75\ \mu\text{m}$ in a tungsten carbide milling vessel, roasted at $1000\ ^\circ\text{C}$ and, after adding 1 g sample to 6 g $\text{Li}_2\text{B}_4\text{O}_7$, fused into a glass bead. Major element analyses were executed on the fused bead using the ARL9400XP+ spectrometer.

Thermogravimetric analysis was conducted on a Mettler Toledo A851 TGA/SDTA device. Powder samples (ca. 10 mg) were placed in open $70\ \mu\text{L}$ alumina pans. Temperature was scanned at $10\ ^\circ\text{C}\ \text{min}^{-1}$ in an air atmosphere from $25\ ^\circ\text{C}$ to $700\ ^\circ\text{C}$.

Infrared spectra were recorded on a Perkin Elmer Spectrum RX I FT-IR system using the KBr method. Data obtained from 32 scans recorded at a resolution of $2\ \text{cm}^{-1}$ were averaged and background-corrected using KBr windows.

Phase identification was carried out by XRD analysis on a PANalytical X-pert Pro powder diffractometer with variable divergence- and receiving slits and an X'celerator detector using Fe-filtered $\text{Co}\ \text{K}\alpha$ radiation ($0.17901\ \text{nm}$). X'Pert High Score Plus software was used for phase identification. Temperature-resolved XRD traces were obtained using an Anton Paar HTK 16 heating chamber with a platinum-heating strip. Scans were measured between $2\theta = 1^\circ$ to 40° in a temperature range of $25\ ^\circ\text{C}$ to $45\ ^\circ\text{C}$ in intervals of $5\ ^\circ\text{C}$ with a waiting time of 1 min and measurement time of 6 min per scan. Si (Aldrich 99% pure) was added to the samples so that the data could be corrected for sample displacement using X'Pert Highscore plus software.

Differential Scanning Calorimetry (DSC) data were collected on a TA Instrument DSC Q100. Samples (5–10 mg) were placed in an alumina pan and heated from $-20\ ^\circ\text{C}$ to $90\ ^\circ\text{C}$ and then

cooled back to $-20\text{ }^{\circ}\text{C}$ at a scan rate of $5\text{ }^{\circ}\text{C min}^{-1}$ and a N_2 flow rate of 50 mL min^{-1} .

Additional DSC scans were recorded on a Mettler Toledo DSC 1 instrument. Approximately 8 mg samples were placed in aluminium pans and pin holes were made in the lids. The samples were heated from $0\text{ }^{\circ}\text{C}$ to $250\text{ }^{\circ}\text{C}$ at a scan rate of $10\text{ }^{\circ}\text{C min}^{-1}$ in N_2 flowing at a rate of 50 mL min^{-1} .

Viscosity measurements were carried out on an Anton Paar MCR 301 Rheometer with a Peltier heating system using a 50 mm parallel plate measuring system with the gap set at 1 mm. Samples (5 g) were placed in the centre of the stationary plate. In isothermal runs the shear rate was increased from 1 s^{-1} to 100 s^{-1} . The effect of temperature on the viscosity was studied at a constant shear rate of 30 s^{-1} unless specified otherwise. The samples were heated from $10\text{ }^{\circ}\text{C}$ to $90\text{ }^{\circ}\text{C}$ and cooled back down to $10\text{ }^{\circ}\text{C}$ at a scan rate of $5\text{ }^{\circ}\text{C min}^{-1}$. The upper limit was chosen as $90\text{ }^{\circ}\text{C}$ as above this temperature the release of intercalated water caused foaming.

Density measurements were carried out using five cycles on a Micrometrics AccuPycII 1340 Helium Gas Pycnometer.

3. Results

3.1. Characterization of LDH-stearates

Unless stated otherwise, all data and information apply to the LDH-stearate that was obtained using an amount of stearic acid equivalent to four times the clay AEC, i.e. LDH-(4)-stearate. Table 1 summarizes selected XRD and TGA data obtained for the various samples. SEM revealed that the LDH- CO_3 consisted of numerous small ($\approx 2\text{ }\mu\text{m}$) inter-grown crystals. Fig. 1 shows that the LDH-(4)-stearate crystals were significantly larger, as much as $10\text{ }\mu\text{m}$ across and that they featured a flake-like morphology. These crystals obtained when using four

times the AEC amount of stearic acid featured irregular surface topography. The change in crystal size and habit indicates that the intercalation was accompanied by recrystallization.

The density measurements with the pycnometer yielded the following values: Jojoba oil 0.86 g cm^{-3} , stearic acid 0.85 g cm^{-3} , LDH-CO₃ 2.25 g cm^{-3} , and LDH-(4)-stearate 1.12 g cm^{-3} .

The bands observed in the FTIR spectrum of the LDH-(4)-stearate (not shown) were consistent with previous investigations [8]. Notable was the absence of a band at 1100 cm^{-1} that is characteristic of the ether functional group present in the polyoxyethylene chains. This indicates that the LDH-(4)-stearate product did not contain any residual Tween 60. FTIR spectra also confirmed the absence of organic material in the product obtained in the absence of the stearic acid. This means that Tween 60 does not intercalate on its own into LDH-CO₃, when using the synthesis procedure described above.

Fig. 2 shows the X-ray diffractograms for stearic acid (99%), LDH-CO₃ and LDH-(4)-stearate prepared with Tween 60 as surfactant at an intercalation temperature of $80 \text{ }^\circ\text{C}$. It also shows a diffractogram for the jojoba oil dispersion containing 30 wt.% LDH-(4)-stearate. The reflection at 0.76 nm ($2\theta = 13.49^\circ$) for LDH-CO₃ was present in the LDH-(4)-stearate and its jojoba oil dispersion confirming that the former was present as a minor phase. The reflections at 4.98 nm ($2\theta = 2.06^\circ$), 2.51 nm ($2\theta = 4.08^\circ$) and 1.68 nm ($2\theta = 6.12^\circ$) are consistent with bilayer intercalated LDH-stearate. The d-spacing of the LDH-stearate, in the 30 wt.% jojoba oil dispersion, was slightly lower being about 4.65 nm .

The TGA traces of all samples (not shown) featured a plateau in the mass loss curves for temperatures beyond $600 \text{ }^\circ\text{C}$. The apparent degree of intercalation of the organo-modified samples was assessed from the relative mass loss values measured at $150 \text{ }^\circ\text{C}$ and $700 \text{ }^\circ\text{C}$ (Table 1) as described by Nhlapo *et al.* [8]. The apparent degree of intercalation of LDH-(4)-stearate was estimated as 3.87 times the anionic exchange capacity (AEC) of the parent clay. This means that almost 96% of the stearic acid added to the reaction mixture was

incorporated in the final product. This value significantly exceeds the maximum theoretical amount of 2.39 times the AEC for close-packed carboxylate chains estimated by Nhlapo *et al.* [8] for this clay. The high stearate content observed suggests that the intercalation procedure may have produced some magnesium stearate and even some aluminium stearate by an acid-base reaction. A complete conversion of the LDH-CO₃ precursor to magnesium distearate and aluminium tristearate would have resulted in an apparent degree of intercalation of 6.93 when using the TGA-determined method blindly.

The XRF results for the LDH-(4)-stearate gave a magnesium to aluminium atom ratio of 2.16 ± 0.05 . This compares favourably with the results for the LDH-CO₃ precursor (2.17 ± 0.06). However, EDS-based determinations revealed wide variations in the magnesium to aluminium ratio for LDH-(4)-stearate. The average was 2.36 with a standard deviation of 0.62. The lowest measured value was 1.44 and the highest 3.16. It is thus safe to say that the reaction product obtained showed rather high variability in the EDS-measured magnesium to aluminium atom ratio while the overall composition is maintained at that of the precursor. Considered together, the EDS, SEM, FTIR, XRF, XRD and TGA data suggest that the reaction most likely resulted in a mixed-layer compound. The data were consistent with the LDH-(4)-stearate comprising approximately 68 wt. % “pure” LDH-stearate with the rest comprising sheets of mixed aluminium and magnesium stearates. Thus the final LDH-(4)-stearate product is perhaps better described as a randomly interstratified clay in which some layers are closer in composition to either magnesium stearate or aluminium stearate. Since the tight packing of these chains is similar to that in stearic acid, it is highly probable that the crystals may even contain isolated layers of dimerized stearic acid sheets.

The LDH-(5)-stearate sample was synthesized in order to explore this possibility. Fig. 3 compares the XRD diffractograms of this product to those of the two precursors. It clearly shows that heating these two soaps together results in a new product (LDH-(5)-stearate) with

a considerably larger d-spacing (5.08 nm) compared to the aluminium stearate (4.01 nm) and slightly larger (4.94 nm) compared to magnesium stearate. TGA data shown in Table 1 indicates that there was a net loss of stearic acid. However, there are also indications in the XRD that not all of the aluminium stearate was converted. Furthermore, it is clear that the product is not a simple LDH-stearate but rather a mixed magnesium-aluminium stearate with a d-spacing that is very similar to that of bilayer-intercalated LDH. This experiment confirmed that such a compound can form by partial hydrolysis of mixtures of the metal stearates. This result supports the assumption that, beyond the conventional LDH-stearate, LDH-(4)-stearate also contained mixed layers of such a product.

3.2. Viscosity of stearic acid suspensions

Fig. 4 shows the stationary shear viscosity of selected jojoba oil LDH-(4)-stearate suspensions as a function of shear rate at a temperature 30 °C. The jojoba oil exhibits Newtonian behaviour as the viscosity is found to be independent of the shear rate. In contrast, the LDH-(4) stearate suspensions show strong shear thinning in the shear rate range from 1 s⁻¹ to 100 s⁻¹. The slopes of the log-log plots varied from -0.73 for the 20 wt.% suspension to -0.79 for the 45 wt.% LDH-(4)-stearate suspension. Fig. 5 shows that a similar shear rate dependence of the apparent viscosity also held at different temperatures. It shows measurements done at 10 °C, 30 °C and 50 °C using the 30 wt.% suspension. The slope changed from about -0.87 at low shear rates to about -0.66 at high shear rates for the shear viscosity measured at 10 °C. The slopes at 30 °C and 50 °C were -0.87 and -0.96 respectively.

Usually one expects the shear viscosity to decrease with the temperature increase. Indeed, a monotonic decrease of viscosity has been observed for the pure jojoba oil. Fig. 6 shows that its viscosity decreases from about 0.04 Pa s at 20 °C to ca. 0.008 Pa s at 90 °C. Surprisingly, a non-monotonic behaviour has been found for the LDH-stearate suspensions upon heating. Fig. 6 and Fig. 7 show that, when suspensions of LDH-stearate are heated, there is an initial decrease in the shear viscosity that reflects the decrease of matrix viscosity. However, one then observes a slight increase in the 20 °C to 40 °C temperature range. At higher temperatures this is again followed by a decrease of viscosity. Fig. 7 shows that a similar viscosity decrease occurs in this range on cooling back to 10 °C. Although Fig. 7 reveals hysteresis for the viscosity response, the viscosities measured between 10 °C and 20 °C of the cooling and heating parts of the cycle coincide for the 20 wt.% suspension. This appears to indicate that the original structure can be fully recovered, at least for this suspension. In contrast, on cooling, the viscosity of the 27 wt.% LDH-(4)-stearate did not fully recover to the initial values during the experimental run.

Fig. 8 shows DSC scans for the 30 wt.% LDH-(4) stearate formulation. A melting endotherm and a crystallization exotherm characteristic of jojoba oil are detected at temperatures below about 12 °C. Particularly significant is the absence of any definitive enthalpy change in the temperature range 25 °C to 40 °C, where the anomalous viscosity behaviour was observed. In addition, temperature-scanned XRD data, previously obtained [8], showed no change in the diffraction patterns up to temperatures of 85 °C. This implies that that the anomalous viscosity increase on heating is not associated with a bulk phase change.

4. Discussion

The Eilers model [12] provides a simple semi-empirical description of the reduced viscosity of a fluid containing suspended flow units:

$$\eta_r = \eta/\eta_o = \{1 + 0.5[\eta] \varphi/(1 - \varphi/\varphi_{max})\}^2 \quad (1)$$

Here η is the viscosity of the suspension; η_o is the viscosity of the neat fluid; η_r is the reduced viscosity; φ is the volume fraction of suspended flow units; φ_{max} is the maximum possible volume fraction of the flow units (corresponds to the randomly close packed situation); and $[\eta]$ is the intrinsic viscosity contributed by the suspended flow units. Both φ_{max} and $[\eta]$ are affected by factors such as the shape of the flow units but only φ_{max} is affected by their size distribution. The flow units correspond to the particles present in the suspension only if they are fully dispersed. For hard spherical particles $[\eta] = 2.5$ and, if they are monodisperse, $\varphi_{max} \approx 0.64$. Care should be taken in defining the flow units. Stable particle agglomerates suspended in the viscous medium effectively trap and immobilize some of the liquid medium in the voids between the particles. In this case the flow units comprise the particle agglomerates together with the immobilized liquid inside them. Since particle agglomerates effectively “solidify” part of the fluid, their action is equivalent to a reduction in the apparent maximum volume fraction fluid units, φ_{max} [13, 14].

The fact that the jojoba oil-LDH-stearate suspensions are shear thinning indicates that the flow units comprise suspended particle agglomerates. Increasing the shear rate generates greater forces acting on these agglomerates. When sufficient shear is applied the agglomerates break down. This releases the entrapped fluid and increases the effective maximum volume fraction particles φ_{max} . The net result is a decrease in the apparent viscosity. If this happens, some of the entrapped liquid is released leading to a reduction in

the viscosity [13-15]. This provides a rationalization of the observed shear thinning shown by the jojoba oil-LDH-stearate suspensions.

The anomalous viscosity increase found on raising the temperature keeping the shear rate fixed can be explained assuming that delamination of the flakes occurs in this temperature range. Here delamination is understood as random splitting of the flakes into two or more parts of microscopic thickness. This is likely since the crystals comprise randomly interstratified layers that differ in composition. Most particles comprise bilayer-intercalated LDH. Thus the individual clay sheets are covered with dense layers of stearic acid on either side. The stearate carboxylic acid head groups associate strongly with the surfaces of the clay sheets via electrostatic and hydrogen bonding interactions. The hydrophobic alkyl chains project outward away from the clay sheets. These “reverse sandwiches” layers are stacked to form the crystalline particles. However, the forces holding them together are essentially weak van der Waals interactions between the tail ends of the stearate molecules on the respective layers. The compositions of the individual sheets differ and this may also imply differences in the surface density and configurations of the stearate molecules. This means that there could be a geometric mismatch at some interfacial layers. This implies weaker bonding between these layers to the extent that at low temperatures the sheets will be so weakly bonded that they may allow facile delamination. This would be especially true if there are sheets of pure neutral stearic acid present in between the stearic acid intercalated clay layers.

Fig. 9 shows a plot of the reduced suspension viscosities vs. temperature additionally normalized with respect to the reduced viscosity measured at 20 °C. It shows that, at low temperatures at least, the normalized viscosity curves coincide. This suggests that the onset of the anomalous viscosity increase is triggered by a thermal event, here assumed to consist of a thermally driven delamination of the particles. Unlike the viscosity curves in Fig. 7 that show a local maximum at ca. 40 °C, the curves in Fig. 9 show a continuous increasing nature. This

means that, while rapid flake delamination commences at ca. 25 °C, it continuous at temperatures above 40 °C albeit at a slower rate.

Fig. 10 shows plots of the reduced viscosity measured at 20.1 °C and 40.1 °C as a function of the volume fraction LDH filler in the suspension. The volume fractions were estimated from the experimental densities of the components. The temperature 20.1 °C corresponds to a point just before the anomalous temperature increase occurs. The temperature 40.1 °C corresponds approximately to the point where the maximum in the viscosity vs. temperature curve is observed. Fig. 10 also shows solid lines that obtained by a least square fit of equation (1) to the experimental data. The parameter values are $[\eta] = 20.4$ and $\varphi_{\max} = 0.471$ for the 20 °C viscosity vs. volume fraction filler curve. The corresponding parameter values for the 40 °C viscosity curve are $[\eta] = 41.8$ and $\varphi_{\max} = 0.569$. These changes can be rationalized as follows. An increase in the intrinsic viscosity is consistent with an increase in the aspect ratio of the flow units. Such a change is expected when the flakes split into two reducing their thickness but maintaining the flake width. Analytical expressions for the intrinsic viscosities of flakes are not presently available. However, at high aspect ratios disc-shaped particles should provide a reasonable approximation. The latter, in turn may be approximated by oblate spheroids. The intrinsic viscosities for oblate spheroids are given by the following equation [15, 16]:

$$[\eta] = \frac{1012 \lambda^3 + 2904 \lambda^2 - 1855 \lambda^{1.5} + 1604 \lambda + 80.44}{1407 \lambda^2 + \lambda} \quad (2)$$

Where the aspect ratio $\lambda = D/t$ is defined as the ratio of diameter D of the oblate spheroid (disc) to its maximum thickness t . Applying this equation (2) to the present experimental results indicates that the aspect ratio was about 26 at 20.1 °C and 56 at 40.1 °C. This result

indicates that the viscosity increase corresponds approximately to a splitting in two of the LDH-(4)-stearate flakes, thereby doubling the aspect ratio.

An increase of 20% in the apparent ϕ_{\max} found on raising the temperature from 20 °C to 40 °C is consistent with a reduction in the degree of particle agglomeration or alternatively, with the partial alignment of the clay flakes parallel to the flow direction. This should provide for a lowering of the overall suspension viscosity. However, the doubling in the apparent intrinsic viscosity apparently overwhelms this effect and a net increase in the viscosity is observed.

5. Conclusions

The nonionic surfactant-assisted intercalation of stearic acid into the carbonate form of a layered double hydroxide yields mixed layer crystals when a large excess of stearic acid is used. The inorganic parts of the sheets show high variability in the aluminium to magnesium atomic ratio. This suggests that the crystals comprise layers that vary from compositions approaching magnesium stearate to those approaching aluminium distearate. This conclusion is supported by the fact that heating a mixture magnesium stearate and aluminium stearate also yielded a new phase with a similar composition. Beyond this, the flakes are also likely to contain interstratified layers of neat stearic acid.

Suspensions of this LDH-stearate in jojoba oil showed complex rheological behaviour. They form weak gels at room temperature when at least 20 wt.% LDH-stearate was present. This implies that at this and higher concentrations the particles present form a space filling network able to support its own weight under gravity. However, when shear is applied this structure breaks down and bulk flow results. The apparent viscosity of the suspensions

showed pronounced shear thinning behaviour indicating sustained breakdown of residual agglomerates as the shear rate is increased. These suspensions also featured an anomalous temperature behaviour. At constant shear rates the viscosity increased by more than a factor of two when the temperature was increased from 25 °C to about 40 °C. This unexpected behaviour is attributed to a temperature driven delamination of primary flake-shaped particles that commences in earnest above 25 °C but it continues, at a lower rate, at temperatures beyond 40 °C. Fitting the semi-empirical Eilers model for the viscosity of particle suspensions to the present data revealed that the delamination improved the effective random packing capacity of the particle agglomerates but that it also increased their aspect ratio. The latter effect dominated leading to the observed viscosity increase when the temperature was raised.

Acknowledgements

This work is based on research supported by the National Research Foundation (NRF) through the Institutional Research Development Programme (IRDP) and the South Africa/Germany Research Collaboration Programme. Financial support from NRF and also from the Bundesministerium für Forschung (BMBF) is gratefully acknowledged.

References

- [1] F. Cavani, F. Trifirò, A. Vaccari, Hydrotalcite-type anionic clays: Preparation, properties and applications, *Catalysis Today*, 11 (1991) 173-301.
- [2] S. Carlino, The intercalation of carboxylic acids into layered double hydroxides: A critical evaluation and review of the different methods, *Solid State Ionics*, 98 (1997) 73-84.
- [3] U. Costantino, F. Marmottini, M. Nocchetti, R. Vivani, New synthetic routes to hydrotalcite-like compounds - Characterisation and properties of the obtained materials, *European Journal of Inorganic Chemistry*, (1998) 1439-1446.

- [4] U. Costantino, M. Nocchetti, M. Sisani, R. Vivani, Recent progress in the synthesis and application of organically modified hydrotalcites, *Zeitschrift fur Kristallographie*, 224 (2009) 273-281.
- [5] D. O'Hare, Inorganic intercalation compounds, in: D.O.H. D. W. Bruce (Ed.) *Inorganic Materials*, John Wiley and Sons, New York, 1991, pp. 166-228.
- [6] F. Leroux, M. Adachi-Pagano, M. Intissar, S. Chauvière, C. Forano, J.P. Besse, Delamination and restacking of layered double hydroxides, *Journal of Materials Chemistry*, 11 (2001) 105-112.
- [7] M. Adachi-Pagano, C. Forano, J.P. Besse, Delamination of layered double hydroxides by use of surfactants, *Chemical Communications*, (2000) 91-92.
- [8] N. Nhlapo, T. Motumi, E. Landman, S.M.C. Verryn, W.W. Focke, Surfactant-assisted fatty acid intercalation of layered double hydroxides, *Journal of Materials Science*, 43 (2008) 1033-1043.
- [9] L. Moyo, N. Nhlapo, W.W. Focke, A critical assessment of the methods for intercalating anionic surfactants in layered double hydroxides, *Journal of Materials Science*, 43 (2008) 6144-6158.
- [10] F.R. Costa, A. Leuteritz, U. Wagenknecht, D. Jehnichen, L. Häußler, G. Heinrich, Intercalation of Mg–Al layered double hydroxide by anionic surfactants: Preparation and characterization, *Applied Clay Science*, 38 (2008) 153-164.
- [11] M.H. El-Mallah, S.M. El-Shami, Investigation of liquid wax components of Egyptian jojoba seeds, *Journal of Oleo Science*, 58 (2009) 543-548.
- [12] H. Eilers, Die Viskosität von Emulsionen hochviskoser Stoffe als Funktion der Konzentration, *Kolloid-Zeitschrift*, 97 (1941) 313-321.
- [13] W.W. Focke, D. Molefe, F.J.W. Labuschagne, S. Ramjee, The influence of stearic acid coating on the properties of magnesium hydroxide, hydromagnesite, and hydrotalcite powders, *Journal of Materials Science*, 44 (2009) 6100-6109.
- [14] C.R. Wildemuth, M.C. Williams, Viscosity of suspensions modeled with a shear-dependent maximum packing fraction, *Rheol Acta*, 23 (1984) 627-635.
- [15] J. Bicerano, J.F. Douglas, D.A. Brune, Model for the viscosity of particle dispersions, *Journal of Macromolecular Science - Reviews in Macromolecular Chemistry and Physics*, 39 C (1999) 561-642.
- [16] J.F.D.a.E.J. Garboczi, Intrinsic viscosity and the polarizability of particles having a wide range of shapes, in: I.P.a.S.A. Rice (Ed.) *Advances in Chemical Physics*, John Wiley & Sons, 1995, pp. 85-153.

LIST OF TABLES

Table 1. Summary of XRD and TGA results for the LDH-CO₃, LDH-stearates and magnesium stearate and aluminium stearate samples.

LIST OF FIG.S

Fig. 1. SEM micrograph showing the flake-like morphology of the LDH-(4)-stearate crystals obtained with Tween 60 as surfactant and four times the AEC amount of stearic acid.

Fig. 2. Arbitrarily scaled X-ray diffractograms for LDH-carbonate, stearic acid, LDH-(4)-stearate and a 30 wt.% dispersion of LDH-(4)-stearate in jojoba oil prepared at a temperature of 80 °C. The corresponding d-spacings were 0.76 nm, 3.97 nm, 4.98 nm and 4.65 nm respectively.

Fig. 3. X-ray diffractograms for magnesium stearate, aluminium stearate and LDH-(5)-stearate prepared via prolonged heating at 70 °C of an aqueous suspension of the former two reagents in the presence of Tween 60.

Fig. 4. The effect of shear rate and LDH-(4)-stearate content on the viscosity of jojoba oil suspensions. The temperature was kept constant at 30 °C.

Fig. 5. The effect of shear rate and temperature on the viscosity of jojoba oil suspensions. The LDH-(4)-stearate content was 30 wt.%.

Fig. 6. The effect of temperature and LDH-(4)-stearate content on the viscosity of jojoba oil suspensions. The shear rate was kept constant at 10 s^{-1} . Temperature was scanned at $5 \text{ }^\circ\text{C min}^{-1}$ from $10 \text{ }^\circ\text{C}$ to $90 \text{ }^\circ\text{C}$.

Fig. 7. The effect of temperature and LDH-(4)-stearate content on the viscosity of jojoba oil suspensions subjected to a heating-cooling cycle. The shear rate was 30 s^{-1} . Temperature was scanned at $5 \text{ }^\circ\text{C min}^{-1}$ from $10 \text{ }^\circ\text{C}$ to $90 \text{ }^\circ\text{C}$ and back. The heating runs are shown in filled symbols and the cooling runs in open symbols.

Fig. 8. DSC trace for a 30 wt. % LDH-(4)-stearate suspension in jojoba oil. Samples were heated at $5\text{ }^{\circ}\text{C min}^{-1}$ from $-40\text{ }^{\circ}\text{C}$ to $90\text{ }^{\circ}\text{C}$ and cooled at the same rate back to $-40\text{ }^{\circ}\text{C}$.

Fig. 9. The effect of temperature and LDH-(4)-stearate content on the relative viscosity normalized with respect to the relative viscosity at $20\text{ }^{\circ}\text{C}$ for each jojoba oil suspensions. The shear rate was 30 s^{-1} and the temperature was scanned at $5\text{ }^{\circ}\text{C min}^{-1}$ from $10\text{ }^{\circ}\text{C}$ to $90\text{ }^{\circ}\text{C}$ and back. The heating runs are shown in filled symbols and the cooling runs in open symbols. LDH-(4)-stearate content: \circ & \bullet = 20 wt.%; \triangle & \blacktriangle = 27 wt.%; and \diamond & \blacklozenge = 40 wt.%.

Fig. 10. The effect of volume fraction filler (LDH-(4)-stearate) on the relative viscosity of jojoba oil suspensions measured during a heating cycle. The shear rate was 30 s^{-1} . The temperature was scanned at $5\text{ }^{\circ}\text{C min}^{-1}$ from $10\text{ }^{\circ}\text{C}$ to $90\text{ }^{\circ}\text{C}$ but only the data obtained at $20.1\text{ }^{\circ}\text{C}$ and $40.1\text{ }^{\circ}\text{C}$ is plotted.

Table 1. Summary of XRD and TGA results for the LDH-CO₃, LDH-stearates and magnesium stearate and aluminium stearate samples.

Sample	d-spacing (nm)	TGA residue* (wt.%)	Degree of intercalation (multiples of AEC)
LDH-carbonate	0.76	59.7	-
LDH-carbonate + Tween 60	0.76	58.4	-
LDH-(2)stearate	4.99	18.22	1.90
LDH-(4)stearate	4.88	9.73	3.48
LDH-(5)stearate	5.08	8.23	5.16
Magnesium stearate	4.94	7.30	5.70**
Aluminium stearate	4.01	8.57	5.11**

*Residual mass at 700 °C relative to the residual mass at 150 °C

**Apparent degree of stearate intercalation expressed as multiples of AEC based on TGA mass loss and assuming that the basis is LDH clay.

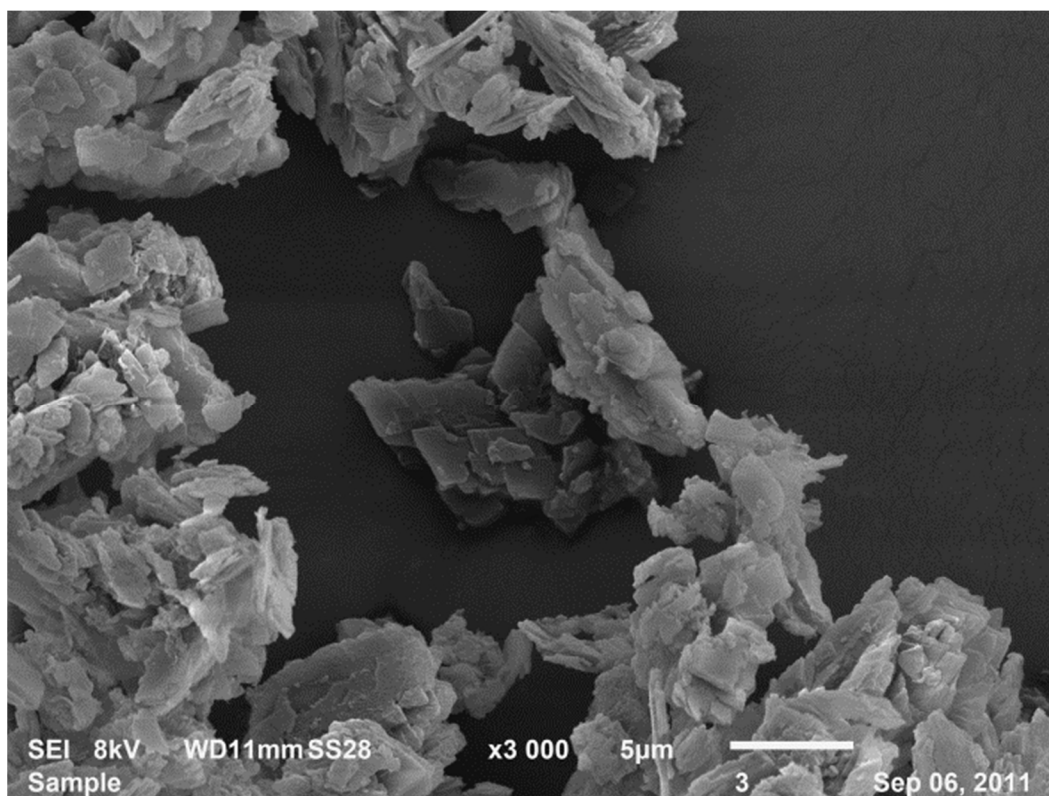


Figure 1. SEM micrograph showing the flake-like morphology of the LDH-(4)-stearate crystals obtained with Tween 60 as surfactant and four times the AEC amount of stearic acid.

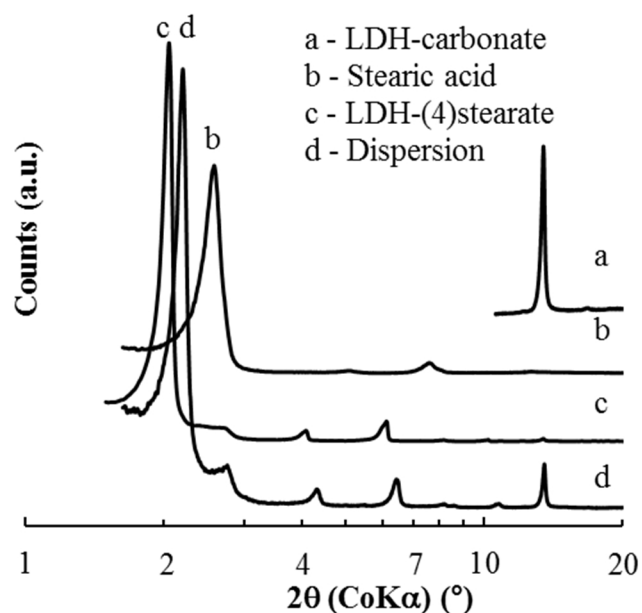


Figure 2. Arbitrarily scaled X-ray diffractograms for LDH-carbonate, stearic acid, LDH-(4)stearate and a 30 wt.% dispersion of LDH-(4)stearate in jojoba oil prepared at a temperature of 80 °C. The corresponding d-spacings were 0.76 nm, 3.97 nm, 4.98 nm and 4.65 nm respectively.

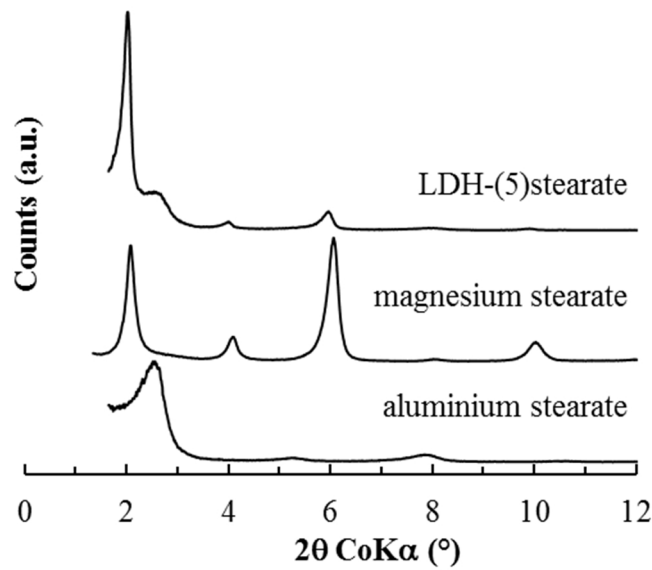


Figure 3. X-ray diffractograms for magnesium stearate, aluminium stearate and LDH-(5)-stearate prepared via prolonged heating at 70 °C of an aqueous suspension of the former two reagents in the presence of Tween 60.

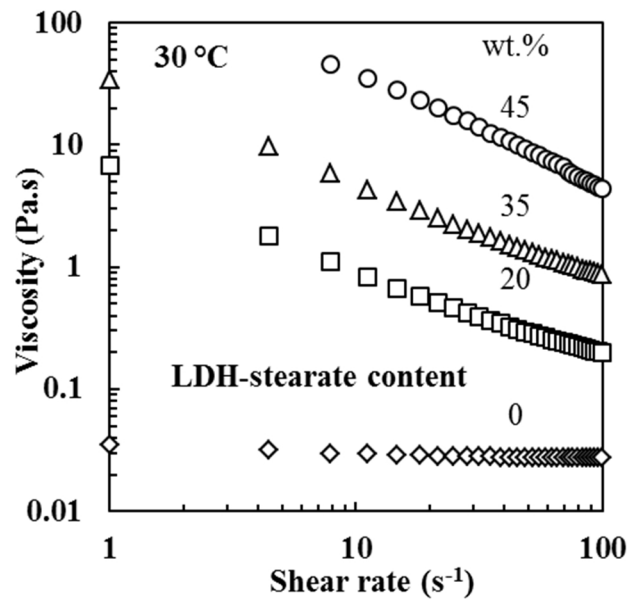


Figure 4. The effect of shear rate and LDH-(4)-stearate-content on the viscosity of jojoba oil suspensions. The temperature was kept constant at 30 °C.

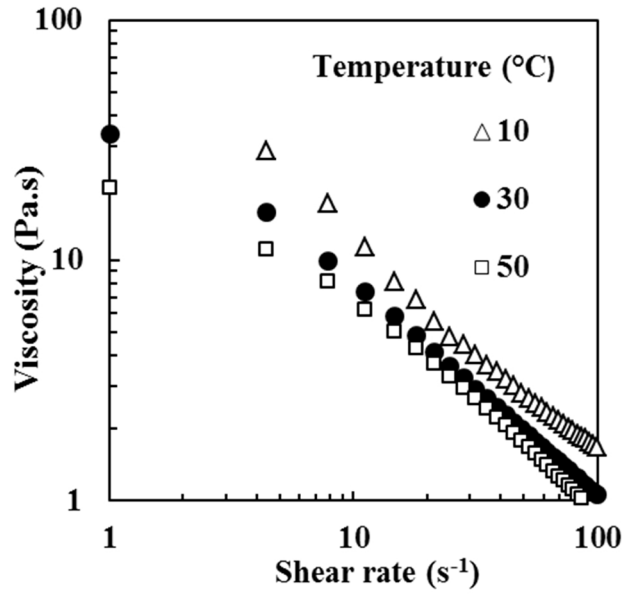


Figure 5. The effect of shear rate and temperature on the viscosity of jojoba oil suspensions. The LDH-(4)-stearate content was 30 wt.%.

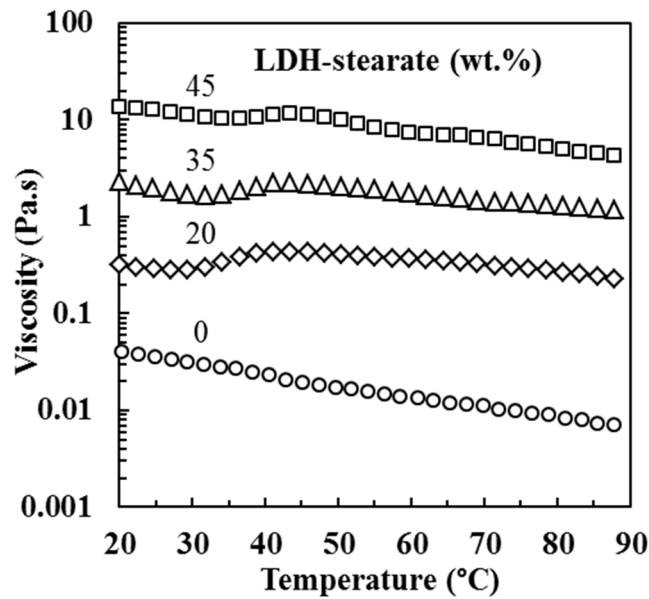


Figure 6. The effect of temperature and LDH-(4)-stearate content on the viscosity of jojoba oil suspensions. The shear rate was kept constant at 10 s^{-1} . Temperature was scanned at $5 \text{ }^\circ\text{C min}^{-1}$ from $10 \text{ }^\circ\text{C}$ to $90 \text{ }^\circ\text{C}$.

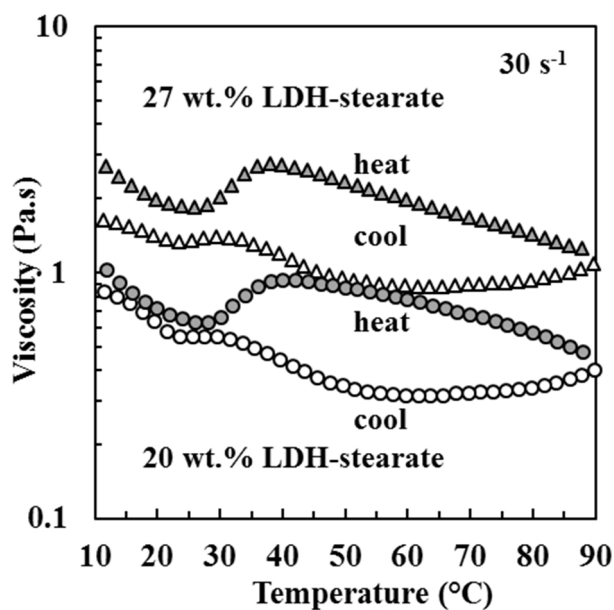


Figure 7. The effect of temperature and LDH-(4)-stearate content on the viscosity of jojoba oil suspensions subjected to a heating-cooling cycle. The shear rate was 30 s^{-1} . Temperature was scanned at $5 \text{ }^\circ\text{C min}^{-1}$ from $10 \text{ }^\circ\text{C}$ to $90 \text{ }^\circ\text{C}$ and back. The heating runs are shown in filled symbols and the cooling runs in open symbols.

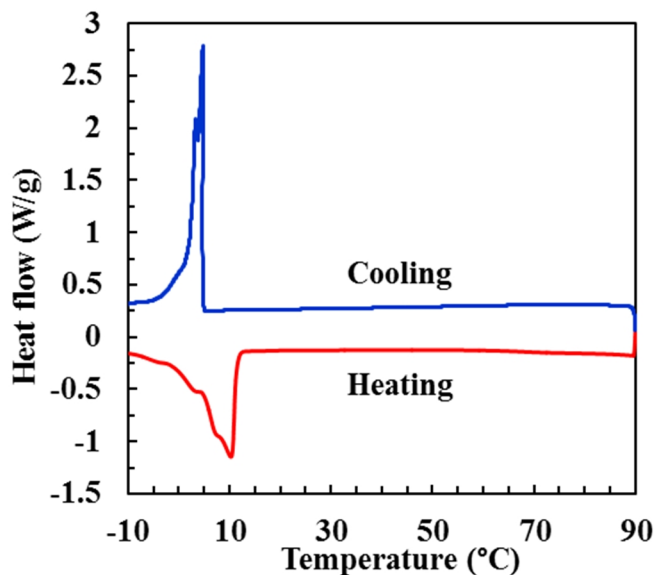


Figure 8. DSC trace for a 30 wt. % LDH-(4) stearate suspension in jojoba oil. Samples were heated at $5 \text{ }^\circ\text{C min}^{-1}$ from $-40 \text{ }^\circ\text{C}$ to $90 \text{ }^\circ\text{C}$ and cooled at the same rate back to $-40 \text{ }^\circ\text{C}$.

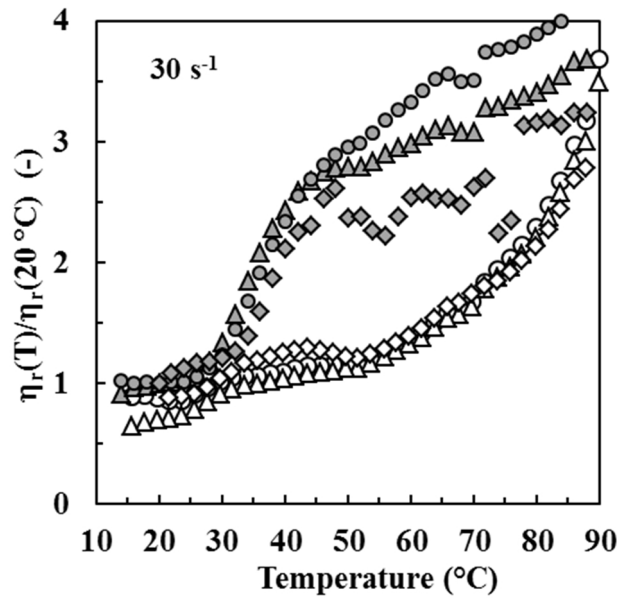


Figure 9. The effect of temperature and LDH-(4)-stearate content on the relative viscosity normalized with respect to the relative viscosity at 20 °C for each jojoba oil suspensions. The shear rate was 30 s^{-1} and the temperature was scanned at $5 \text{ }^\circ\text{C min}^{-1}$ from 10 °C to 90 °C and back. The heating runs are shown in filled symbols and the cooling runs in open symbols. LDH-(4)stearate content: \circ & \bullet = 20 wt.%; \triangle & \blacktriangle = 27 wt.%; and \diamond & \blacklozenge = 40 wt.%. Solid and open symbols indicate heating and cooling runs respectively.

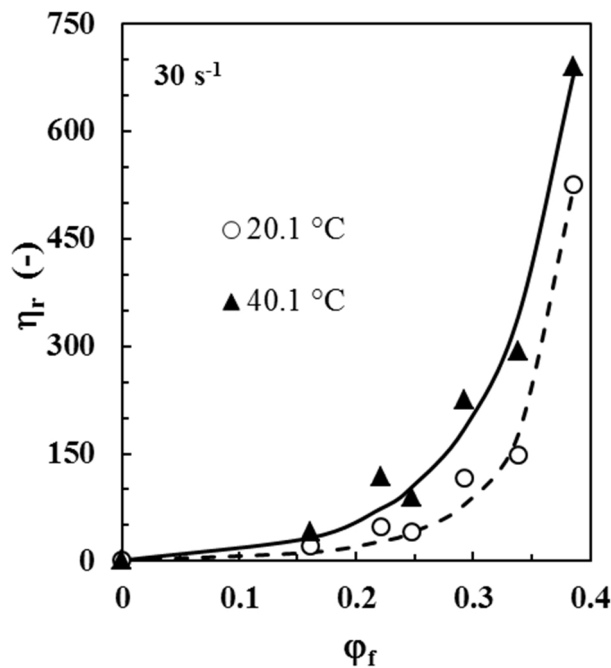


Figure 10. The effect of volume fraction filler (LDH-(4)-stearate) on the relative viscosity of jojoba oil suspensions measured during a heating cycle. The shear rate was 30 s^{-1} . The temperature was scanned at $5 \text{ }^\circ\text{C min}^{-1}$ from 10 °C to 90 °C but only the data obtained at 20.1 °C and 40.1 °C is plotted.